Structural and defect characterization of GaAs and $Al_xGa_{1-x}As$ grown at low temperature by molecular beam epitaxy

S. Fleischer,[a] C. D. Beling, and S. Fung
Department of Physics, University of Hong Kong, Pokfulam Road, Hong Kong

W. R. Nieveen, J. E. Squire, and J. Q. Zheng
Material Characterisation and Preparation Centre, Hong Kong University of Science and Technology, Clearwater Bay Road, Kowloon, Hong Kong

M. Missous
Department of Electrical Engineering and Electronics and Centre for Electronic Materials, University of Manchester Institute of Science and Technology, Manchester M60 1QD, United Kingdom

(Received 8 July 1996; accepted for publication 27 September 1996)

We have investigated the structural and defect characteristics of GaAs and $Al_xGa_{1-x}As$ grown at low substrate temperature (250 °C) by molecular beam epitaxy. Using x-ray diffraction we have observed an increase in lattice parameter for all as-grown layers, with the $Al_xGa_{1-x}As$ layers showing a smaller expansion than the GaAs layer. However, infrared absorbtion measurements revealed that the concentration of neutral arsenic antisite defect, $[As_{Ga}]^0$, was not significantly affected by aluminum content (x), with only a small reduction for $x=0.36$. Positron beam studies showed that the low temperature layers had a higher concentration of vacancy-related defects ($\sim 10^{17}$ cm^{-3}) than the semi-insulating substrate, with the $Al_xGa_{1-x}As$ layers having the highest values. After annealing (600 °C, 15 min) the lattice constants relaxed to those of conventionally grown material and $[As_{Ga}]^0$ was reduced in all cases, with the smallest reduction occurring for the $x=0.36$ layer, indicating that the Al atoms strengthen the lattice against excess arsenic incorporation and hold the arsenic antisite atoms more strongly in position. X-ray photoelectron spectroscopy showed that arsenic diffused out of the surface region and was replaced by oxygen, possibly due to an insufficient overpressure of forming gas during the anneal. This oxygen penetration was greater for the GaAs layer than for the $Al_xGa_{1-x}As$ layers. Extra Raman peaks at 200 and 257 cm^{-1} confirmed that the surface was very disordered. There was, nevertheless, a large increase (4%) in the positron S parameter in the bulk of the annealed layers, suggesting the formation of vacancy clusters, whereas in the surface region we find evidence that As_{Ga} diffusion proceeded at a faster rate in the $x=0.36$ than the $x=0.2$, in agreement with the vacancy-enhanced As_{Ga} diffusion model. © *1997 American Institute of Physics.* [S0021-8979(97)04401-0]

I. INTRODUCTION

Over the last several years considerable interest has been shown in GaAs layers grown by molecular beam epitaxy (MBE) at low substrate temperatures (200–300 °C).[1–8] Although the growth of low-temperature GaAs (LT-GaAs) was first reported by Murotani *et al.* in 1978,[9] this interest stems, to a large extent, from a 1988 paper by Smith *et al.*[10] Whereas the former work suggested that LT-GaAs might find use as a highly resistive buffer layer for GaAs integrated circuits, it was the latter study that demonstrated that backgating could be eliminated by inserting a LT layer between the device and the substrate. However, LT-GaAs is also interesting from a purely scientific standpoint. In its as-grown form, LT-GaAs exhibits an increased lattice parameter due to the incorporation of excess arsenic during growth. Yu *et al.*[11] have shown that at a substrate temperature of 190 °C the lattice constant is increased by ~0.14%. Particle-induced x-ray emission (PIXE) data by the same authors show that this corresponds to an increased As concentration, Δ[As], of ~1.5 at. % ($\approx 6.6\times 10^{20}$ cm^{-3}). Increasing the growth temperature to 300 °C reduced the lattice constant increase to <0.01%, the detection limit of the x-ray rocking curve measurements, with an off-stoichiometry Δ[As] of <0.1 at. %. They estimated, using PIXE/channeling, that approximately 60% of the excess As was located in the interstitial position, with the remainder forming arsenic antisite defects, As_{Ga}. Further, the interstitial As was shown to be located close to normal As sites and not in exact interstitial positions. Electrically, as-grown LT-GaAs exhibits high resistivity ($\sim 10^4$–10^5 Ω cm) and this has been reported to be due to ''hopping'' conduction between closely spaced As antisites.[12]

Annealing studies[13,14] have revealed that the increased lattice parameter of LT-GaAs begins to reduce upon heating to 300 °C, and returns to the ''normal'' value at temperatures greater than ~550 °C. The As_{Ga} defect concentration $[As_{Ga}]$ also reduces on annealing,[15] while positron beam measurements[16–18] indicate a rise in vacancy-related defects. Arsenic outdiffusion during annealing can be minimized by keeping the samples in an As (or neutral gas) overpressure, and transmission electron microscopy (TEM) studies have shown that the excess arsenic forms precipitates.[19] The resistivity of annealed LT-GaAs has been observed to increase to $\sim 10^8$ Ω cm,[20] and this has been attributed to a reduction in

[a]Electronic mail: sfleisch@hkucc.hku.hk

 0021-8979/97/81(1)/190/9/$10.00 © 1997 American Institute of Physics

Downloaded¬09¬Nov¬2006¬to¬147.8.21.97.¬Redistribution¬subject¬to¬AIP¬license¬or¬copyright,¬see¬http://jap.aip.org/jap/copyright.jsp

hopping conduction since this form of conduction decreases exponentially with increased trap center separation.

There has been relatively little work on $Al_xGa_{1-x}As$ grown at low temperature to date. It was found[21] that this material, when annealed, has a much higher resistivity than annealed LT-GaAs (up to four orders of magnitude greater or $\sim 10^{12}$ Ω cm). Mahalingham *et al.*[22] investigated superlattices of GaAs/$Al_xGa_{1-x}As$ grown at low temperature and reported that annealing causes the excess arsenic to diffuse from the $Al_xGa_{1-x}As$ layers into the GaAs layers. Meanwhile, Verma *et al.*[23] found that the dilation of the lattice constant in the as-grown material was a decreasing function of aluminum content, while a study of magnetic circular dichroism of absorption (MCDA)[24] in LT-$Al_xGa_{1-x}As$ revealed a high concentration of $[As_{Ga}]^+$, the paramagnetic form of the arsenic antisite defect. Nonetheless, there are still many unanswered questions regarding the effects of the aluminum mole fraction on defect concentrations and on precipitate formation. Therefore, in this work we have used a variety of experimental techniques to investigate both LT-GaAs and LT-$Al_xGa_{1-x}As$ with the aim of correlating their structural properties to their defect concentrations. High-resolution x-ray diffraction and Raman spectroscopy were employed to study the structure of these materials, whereas Fourier-transform infrared (FTIR) absorption and positron annihilation spectroscopy were used to characterize their defect profiles. Finally, chemical information as a function of depth below the surface were obtained from x-ray photoelectron spectroscopy (XPS). To our knowledge, it is the first time that Raman, FTIR, XPS and positron techniques were used to study LT-$Al_xGa_{1-x}As$.

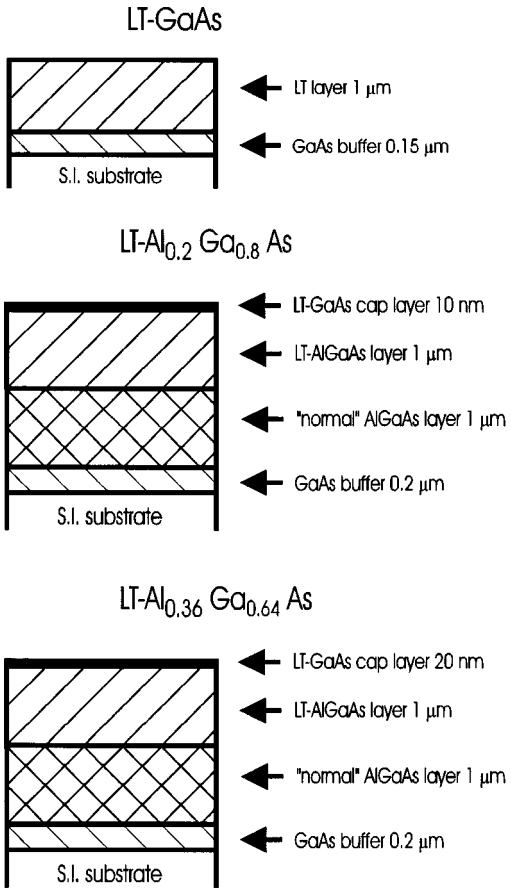

FIG. 1. Schematic diagrams of the samples used in this study.

II. EXPERIMENT

The epitaxial layers used in this study were all grown in a Vacuum Generators V90H MBE system on (100) semi-insulating liquid-encapsulated Czochralski (SILEC) GaAs wafers using indium-free mounting. Solid arsenic (7N grade) was used to generate the tetramer species (As_4) and the growth rate was 1 μm/h. The beam equivalent pressure (BEP) ratios were measured using a nude ion gauge near to the growth position and were found to be 6 for all samples. Annealing was subsequently carried out at 600 °C for 15 min. In order to minimize the loss of arsenic from the lattice, each sample was sandwiched between two pieces of undoped GaAs substrate and maintained in a forming gas (20% hydrogen: 80% nitrogen) overpressure. The structures of the three samples investigated for this work are shown schematically in Fig. 1. The first sample consisted of a 1500 Å buffer layer and a 1 μm undoped LT-GaAs epilayer. The $Al_xGa_{1-x}As$ alloy structures were both essentially the same apart from a slight variation in the cap layer, and consisted of a GaAs buffer layer, a 1 μm alloy layer grown at ''normal'' temperature, followed by a similar thickness of LT-grown alloy. The LT-GaAs cap was grown to protect the reactive $Al_xGa_{1-x}As$ alloy. All LT layers were grown at 250 °C, whereas the normal growth temperature was 580 °C for the $x=0.2$ alloy and 600 °C for the $x=0.36$ alloy. Above 400 °C the growth temperature was calibrated using an Ircon Modline Plus infrared pyrometer. Below 400 °C the growth temperature was determined by extrapolation from readings taken from a thermocouple located close to the substrate.

High-resolution x-ray diffraction (HRXRD) studies were carried out using a Philips PW1825 diffractometer. Using Cu $K_{\alpha 1}$ line radiation (1.54056 Å) and a four-crystal Bartels monochromator, the lattice constant for the (001) direction was determined, assuming a substrate lattice constant of 5.6533 Å.[25] Stokes-mode Raman spectra were acquired using a Renishaw System 3000 Raman imaging microscope (Ramascope). Using backscattering geometry, the incident light from a helium–neon laser (25 mW, 633 nm) was focused onto the sample surface with a spot size ~ 1 μm. The penetration depth was estimated to be ~ 500 nm, ensuring that the Raman spectra were characteristic of the LT layers only.

Room temperature near-band-edge infrared absorption measurements were carried out using a Bio-Rad FTS6000 fast-Fourier transform infrared spectrometer and a UMA500 microscope with a HgCdTe detector cooled to 77 K. The concentration of neutral antisite-related defects was calculated from the absorption coefficient at 1.24 eV, after subtracting the background absorption at 0.6 eV and making a correction for the EL2 concentration of the substrate (taken as 7×10^{15} cm^{-3}).[26] The 5 K calibration published by Martin[27] was then used to relate the absorption coefficient to the EL2 concentration. The detection limit of the neutral antisite defect concentration was estimated to be $\sim 10^{18}$ cm^{-3}.

Downloaded¬09¬Nov¬2006¬to¬147.8.21.97.¬Redistribution¬subject¬to¬AIP¬license¬or¬copyright,¬see¬http://jap.aip.org/jap/copyright.jsp

XPS was carried out using a Physical Electronics surface science analysis system (model PHI 5600) with a custom preparation chamber. Three kV argon atoms were used to sputter the surface at a rate of between 15 and 25 Å/min, and aluminum K_α x rays (1486.6 eV) produced the O $1s$, Ga $2p3$, As $3d$, and Al $2p$ peaks.

Positron beam measurements were performed with a variable energy slow-positron beam that has a beam diameter of ~8 mm and a maximum implantation energy of 30 keV. Positrons from a ^{22}Na source (30 mCi) were moderated by a tungsten single crystal (100) in order to produce a monoenergetic beam (~3 eV). After moderation the positrons were transported and focused by magnetic field and accelerated to achieve the required implantation depth. After rapidly thermalizing ($<10^{-11}$ s), the positrons diffuse (in the absence of an electric field) until annihilating with an electron, producing two gamma ray (511 keV) photons that are detected by a high-purity germanium (HPGe) detector. The detector resolution was 1.26 keV at 511 keV. For this work, annihilation line shape spectra (5×10^5 counts) were accumulated at energies ranging from 0.5 to 15 keV, which correspond to a maximum mean implantation depth of ~0.57 μm.[28] The annihilation spectrum was characterized by the S parameter, which is defined as the area under the central part of the annihilation photopeak divided by the total area.[29] The absence of ion cores at vacancy-type defects means that these sites act as trapping sites for positrons. Annihilation with low energy valence electrons at these defects results in a narrowing of the photopeak, corresponding to an increase in the S parameter.

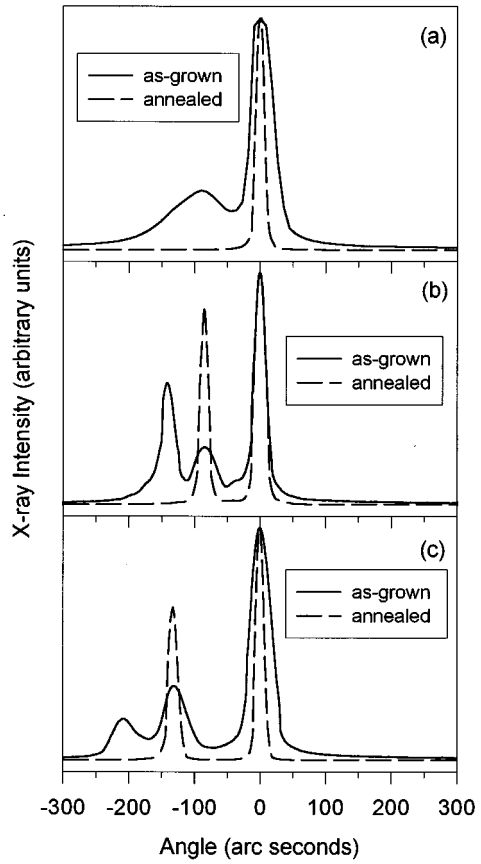

FIG. 2. X-ray rocking curves for (a) LT-GaAs, (b) LT-$Al_{0.2}Ga_{0.8}As$, and (c) LT-$Al_{0.36}Ga_{0.64}As$ samples. Epilayer peak intensities were normalized to the substrate peak intensity.

III. RESULTS AND DISCUSSION

A. Structural characterization

In Fig. 2(a), the x-ray rocking curve for the as-grown LT-GaAs shows two peaks characteristic of the GaAs substrate (at the zero position) and the strained low-temperature layer that is shifted by −0.0259°. This corresponds to a relative lattice expansion of 0.0785%. For the case of the $Al_xGa_{1-x}As$ alloy [Fig. 2(b), $x=0.2$), three peaks can be observed, namely, the substrate (0°), the ''normal'' $Al_xGa_{1-x}As$ layer (−0.0235°) which itself is lattice mismatched from the substrate, and the LT-$Al_xGa_{1-x}As$ (−0.0394°). Similarly, the values for the $x=0.36$ sample [Fig. 2(c)] are ''normal'' (−0.0365°) and LT (−0.0578°). The difference in peak positions for the normal layers in Figs. 2(b) and 2(c) yield Al mole fractions of $x=0.22$ and $x=0.35$, respectively, which is in good agreement with nominal growth values. In contrast, the rocking curves after annealing illustrate the relaxation of the lattice that takes place due to the redistribution of the excess arsenic. Now, the LT-GaAs peak has disappeared, as have the LT-$Al_xGa_{1-x}As$ peaks leading to enhanced normal $Al_xGa_{1-x}As$ peak intensities.

In order to compare our results with those of other researchers, we have plotted the relative lattice expansion (of the low-temperature layer relative to the normal layer) as a function of aluminum mole fraction (Fig. 3). For GaAs ($x=0$), we find that our value of 0.0785% agrees extremely well with Liliental-Weber *et al.*[13] (0.79%), and follows the general trend observed by others[11,14] that the relative lattice mismatch decreases with increasing growth temperature. The only x-ray results for LT-$Al_xGa_{1-x}As$ prior to this work were published by Verma *et al.*[23] who examined epitaxial

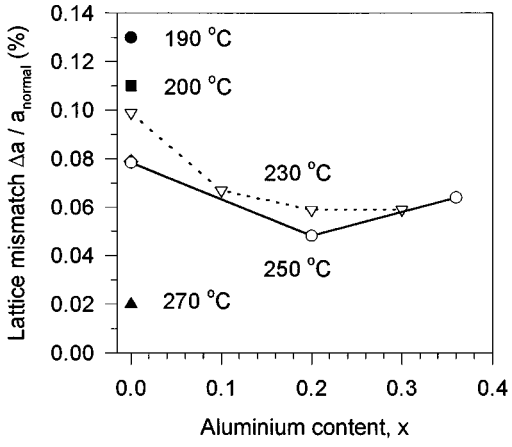

FIG. 3. Lattice mismatch (of the LT layers relative to the ''normal'' values) as a function of Al mole fraction. Data for 190, 200, and 270 °C are from Ref. 6; 230 °C (connected with dotted line) is from Ref. 17; 250 °C (solid symbol) is from Ref. 8. Open symbols connected with solid line are results from this investigation.

Downloaded¬09¬Nov¬2006¬to¬147.8.21.97.¬Redistribution¬subject¬to¬AIP¬license¬or¬copyright,¬see¬http://jap.aip.org/jap/copyright.jsp

films grown at 230 °C. Their data are plotted in Fig. 3 and it can be seen that the introduction of Al leads to a reduction in relative lattice expansion. These authors observed that for an Al content greater than 0.2 the expansion reached a minimum value of 0.059%. Our values show a reduced mismatch consistent with our higher growth temperature (250 °C) and, although the $x=0.36$ sample shows an increase in $\Delta a/a_{\text{normal}}$ when compared to the $x=0.2$ sample, both sets of data show similar behavior, namely, that the introduction of Al reduces the relative lattice mismatch for any given substrate temperature. Verma *et al.* conjectured that this was due to a diffusion process similar to that reported by Mahalingam *et al.*,[22] who observed that the excess arsenic at the interfaces of an LT-GaAs/$Al_xGa_{1-x}As$ superlattice diffused out of the $Al_xGa_{1-x}As$ and into the GaAs during annealing. This was attributed to an increased chemical potential for As in the Al-containing layers; and Verma *et al.* speculated that their results could be explained if a similar process operated at the $Al_xGa_{1-x}As$ surface during growth. However, in a later investigation[30] a new mechanism was proposed for the superlattice data, one in which the incubation time for the formation of As precipitates was longer in the $Al_xGa_{1-x}As$ layers than in the GaAs layers. After a certain anneal time this would cause an As concentration gradient across the interfaces resulting in a diffusion of As from the $Al_xGa_{1-x}As$ layers into the GaAs. This new mechanism, based on precipitate formation, cannot explain the as-grown data. Yet if a diffusion process based on chemical potentials is in operation, then this should result in a reduction in the concentration of arsenic-related defects $[As_{Ga}]^0$ for increasing aluminum concentration. Measurements of $[As_{Ga}]^0$ are presented in Sec. III B.

Raman spectroscopy is now widely used to examine a number of semiconductor characteristics,[31] but little work has been done on GaAs grown at low temperature,[32] and none to our knowledge on LT-$Al_xGa_{1-x}As$. In essence, laser light is focused onto the sample by way of an optical microscope that also collects the scattered light and transmits it to a spectrometer. We have employed Raman microprobe spectroscopy in order to investigate the crystalline quality of LT-grown layers, and Fig. 4 shows the spectra for all three as-grown samples. The penetration depth of the 633 nm laser light was calculated from the relation $\lambda/2\pi k$, where k is the extinction coefficient and is estimated to be ~480 nm, confirming that the spectra obtained were characteristic of the LT layers only. For the case of LT-GaAs the sharp peak at 291 cm^{-1} corresponds to the longitudinal optical (LO) phonon at the Γ critical point located at the center of the Brillouin zone. The smaller peak at 268 cm^{-1} is attributed to the transverse optical (TO) phonon, which is forbidden by the selection rules for (100) backscattering geometry. The appearance of the TO phonon peak could be due to a deviation of the incident laser light form the surface normal[31] or to the large collection angle used by the Ramascope.[33] However, since these factors do not change from sample to sample, and the relative intensities of the TO peak to the LO peak do change, we attribute the appearance of the TO peak to crystalline disorder normal to the substrate (001). For the case of the $Al_xGa_{1-x}As$ alloys we find a typical two-mode phonon

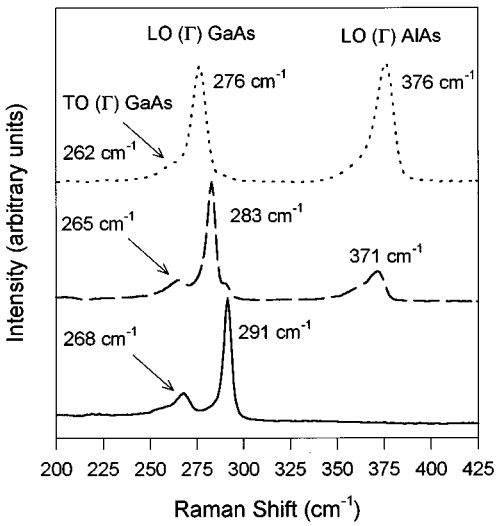

FIG. 4. Raman spectra for the as-grown samples: LT-GaAs (solid line); LT-$Al_{0.2}Ga_{0.8}As$ (dashed line); and LT-$Al_{0.36}Ga_{0.64}As$ (dotted line).

spectrum, with two sets of optical frequencies associated with GaAs and AlAs, where the intensities are indicative of the relative concentrations.[25] In addition, the LO and TO peaks are shifted in frequency due to compositional changes, and these shifts are in good agreement with published values.[34] Hence, we find no difference in the Raman characteristics between the LT layers and those of layers grown at conventional MBE temperatures.

The Raman spectra for the three annealed samples (Fig. 5) are quite distinct from those of the as-grown samples. Now two extra peaks, situated at ~257 and ~200 cm^{-1} for LT-GaAs, can be seen, that moving to lower values (254 and 195 cm^{-1} for $x=0.36$) for increasing Al mole fraction. The peak at ~257 cm^{-1} is due to the TO phonon at the Brillouin zone edge (X), whereas the peak at ~200 cm^{-1} is thought to be associated with longitudinal acoustic (LA) phonon at the (L) point.[25] These additional peaks in the annealed samples also cannot be explained using Raman scattering theory applied to the (100) backscattered surface, and are believed to be disorder induced. Jusserand and Sapriel[35] studied epitaxial $Al_xGa_{1-x}As$ and found evidence for similar peaks which they suggested were due to acoustic phonons that become Raman active as a result of disorder which is produced by aluminum atoms substituting gallium atoms in the gallium sublattice. In our case, it should be noted that the annealed samples did not have uniformly smooth and mirrorlike surfaces but had darker, unreflective patches indicating some problem with the annealing process. The layers were probed in a number of positions and the additional disorder-induced peaks were not always in evidence; the spectrum in some locations closely resembled that of the as-grown case. Although we initially thought these extra peaks might be due to areas of high As precipitate concentration, we now attribute them, in the light of the XPS data, to a high degree of disorder at the surface of the samples due to outdiffusion of arsenic and penetration of oxygen. More details of the XPS measurements are given at the end of Sec. III B, and a more detailed Raman study is planned in the future.

Downloaded¬09¬Nov¬2006¬to¬147.8.21.97.¬Redistribution¬subject¬to¬AIP¬license¬or¬copyright,¬see¬http://jap.aip.org/jap/copyright.jsp

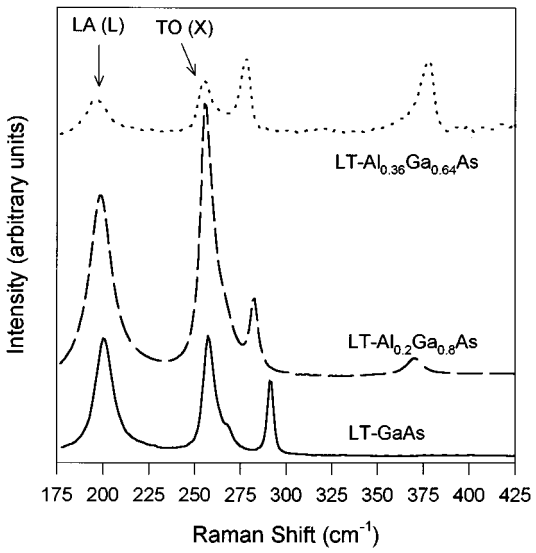

FIG. 5. Raman spectra for the annealed samples showing the extra disorder-induced peaks at ~200 and ~257 cm^{-1}.

B. Defect characterization

The reduction in the relative lattice expansion as the Al mole fraction increases from $x=0$ to $x=0.36$, demonstrated by the x-ray rocking curve data in Fig. 3, indicates that the introduction of Al reduces the incorporation of excess As into the LT layers, possibly due to the strengthening of the lattice by the Al–As bond. Therefore, the concentration of neutral antisite defects $[As_{Ga}]^0$ might be expected to decrease with increasing Al, and FTIR absorption measurements were performed in order to test this hypothesis. However, the graph of absorbance against photon energy [Figs. 6(a)–6(c)] shows that there is no detectable difference in absorbance between the as-grown LT-GaAs and LT-$Al_{0.2}Ga_{0.8}As$ layers, whereas the absorbance for the as-grown LT-$Al_{0.36}Ga_{0.64}As$ layer is markedly lower. The calculated values for $[As_{Ga}]^0$ (at a photon energy of 1.24 eV) are found to be LT-GaAs (2.7×10^{19} cm^{-3}), LT-$Al_{0.2}Ga_{0.8}As$ (2.7×10^{19} cm^{-3}), and LT-$Al_{0.36}Ga_{0.64}As$ (1.7×10^{19} cm^{-3}), with the LT-GaAs results being in good agreement with the work of others.[36] After annealing the $[As_{Ga}]^0$ decreases to 8.7×10^{18} cm^{-3} for LT-GaAs, 9.5×10^{18} cm^{-3} for LT-$Al_{0.2}Ga_{0.8}As$, and 1.1×10^{19} cm^{-3} for LT-$Al_{0.36}Ga_{0.64}As$. These results are summarized in Table I. Taken as a percentage decrease, it can be seen that the reduction in neutral arsenic antisite defect concentration due to annealing for the LT-$Al_{0.36}Ga_{0.64}As$ sample is only 35% compared to 68% and 65% for the other two samples. This would seem to be consistent with the proposal of Mahalingam *et al.*[30] that precipitate formation is slower in $Al_xGa_{1-x}As$ than in GaAs, with the condition that an Al mole fraction greater than 0.2 is necessary to have a measurable effect on the retardation of precipitate formation.

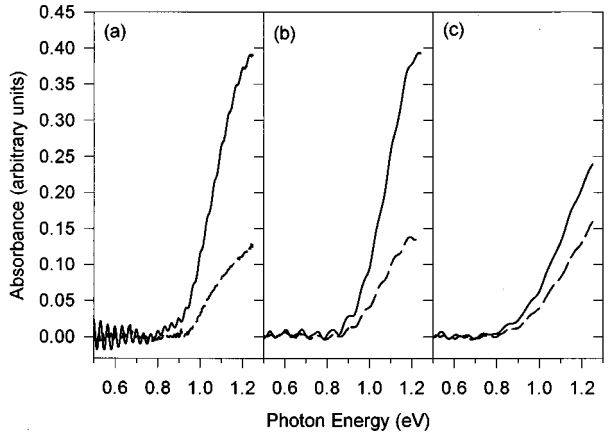

FIG. 6. FTIR absorbance spectra for the three samples: (a) LT-GaAs, (b) LT-$Al_{0.2}Ga_{0.8}As$, and (c) LT-$Al_{0.36}Ga_{0.64}As$. Solid lines are for as-grown data; dashed lines are for annealed data.

TABLE I. Neutral arsenic antisite concentrations for the as-grown and annealed layers as a function of aluminum mole fraction.

Al mole fraction	$[As_{Ga}]^0$ ($\times10^{19}$ cm^{-3})		
(%)	As-grown	Annealed	Decrease (%)
0	2.7	0.87	68
20	2.7	0.95	65
36	1.7	1.1	35

Based on the calibration of Yu *et al.*[11] it is possible to estimate the concentration of excess As from the lattice mismatch data. The results show that the off-stoichiometric As concentration $\Delta[As]$ is $\sim3.5\times10^{20}$ cm^{-1} for LT-GaAs, 2.7×10^{20} cm^{-1} for LT-$Al_{0.2}Ga_{0.8}As$, and 3.2×10^{20} cm^{-1} for LT-$Al_{0.36}Ga_{0.64}As$. The reason for the increased concentration for the $x=0.36$ layer (when compared to $x=0.2$) is not known, but is indicative of a lower than intended growth temperature. It is difficult to measure the substrate temperature accurately in the LT regime and a difference of only a few degrees would have a large effect on $\Delta[As]$. However, to our knowledge, there have been no other studies of Al fractions greater than $x=0.3$, and it is possible that a new mechanism exists in this regime that inhibits excess arsenic incorporation. Table II summarizes the $\Delta[As]$ and as-grown $[As_{Ga}]^0$ concentrations, and it is apparent that less than 10% of the excess arsenic is in the form of the neutral antisite defect. Electron paramagnetic resonance (EPR) studies of LT-GaAs have shown[37] that the concentration of the single-ionized antisite defect, $[As_{Ga}]^+$, is of the order of 10^{18} cm^{-3}, which is only about one-tenth of the concentration of the defect in its neutral state. Since the excess As can either be incorporated in the lattice as antisite defects, As_{Ga}, or as interstitials, As_i,[38] it is possible to estimate the percentage of the As at each location. The results for the three as-grown

TABLE II. Excess arsenic and neutral arsenic antisite concentrations as a function of aluminum mole fraction.

Al mole fraction (%)	$\Delta[As]$ ($\times10^{20}$ cm^{-3})	As-grown $[As_{Ga}]^0$ ($\times10^{19}$ cm^{-3})	Antisite fraction (%)
0	3.5	2.7	8
20	2.7	2.7	10
36	3.2	1.7	5

Downloaded¬09¬Nov¬2006¬to¬147.8.21.97.¬Redistribution¬subject¬to¬AIP¬license¬or¬copyright,¬see¬http://jap.aip.org/jap/copyright.jsp

layers are as follows: LT-GaAs (~92% interstitial, ~8% antisite), LT-$Al_{0.2}Ga_{0.8}As$ (~90%, ~10%), and LT-$Al_{0.36}Ga_{0.64}As$ (~95%, ~5%), which is considerably different from the 60% interstitial value reported by Yu *et al.*[11] Given that these estimates are based on an interpolation of only four data points, we conclude that there is no significant difference in the location of the excess arsenic as a function of Al content.

Variable energy positron beam spectroscopy has been widely used as a nondestructive, depth-profiling probe of vacancy-related defects in condensed matter.[29] Upon implantation into the solid the positrons lose most of their kinetic energy (thermalize) within a few picoseconds and then diffuse until annihilating with an electron. The positron implantation or ''stopping'' profile, $P(E,z)$, is defined as the depth distribution of the positrons after they have thermalized and is given by the Makhov function[39]

$$P(E,z) = -\frac{d}{dz}\exp\left[-\left(\frac{z}{z_0}\right)^m\right], \tag{1}$$

where z is the depth and m is the shape parameter that is usually taken to be 2. The depth parameter, z_0, is a function of the mean implantation depth, $\bar{z}$, which is given by

$$\bar{z} = \frac{A}{\rho}E^n, \tag{2}$$

where A and n are constants (taken to be 400 Å g cm^{-3} keV^{-n} and 1.6, respectively), ρ is the density (g/cm^3), and E is the energy (in keV).[28] The Doppler broadening of the annihilation line shape, characterized by the S parameter, is a measure of the electron momentum distribution at the annihilation site. The measured S parameter is actually a linear superposition of contributing S parameters from the surface and the bulk for the case of a single layer system and can be expressed as

$$S(E) = S_{\text{surf}} f_{\text{surf}}(E) + S_{\text{bulk}}[1 - f_{\text{surf}}(E)], \tag{3}$$

where $f_{\text{surf}}(E)$ is the fraction of positrons annihilating at the surface, or more generally for a multilayer system as

$$S(E) = S_{\text{surf}} f_{\text{surf}}(E) + \sum_i S_i f_i(E), \tag{4}$$

where i denotes the ith layer. The computer program VEPFIT[40] was used to fit the experimental data by analyzing the energy dependence of the S parameter.

Figure 7 shows the S parameter (normalized to the substrate bulk value) versus positron implantation energy data for both the as-grown and and annealed samples. Since the highest beam energy used was ~15 keV, corresponding to a maximum mean penetration depth of ~0.6 μm, essentially all of the positrons can be considered to be annihilating in the LT layers (1 μm). Clearly all of the as-grown LT layers show an increased S parameter when compared to the substrate, with LT-GaAs showing the smallest increase (~0.8%) and the $Al_xGa_{1-x}As$ alloys exhibiting virtually the same higher values (~1.5%). These values are in good agreement with accepted trapping levels from monovacancies.[41] Furthermore, the positrons that are implanted into the LT layers beyond ~0.1 μm produce a constant S parameter, indicating

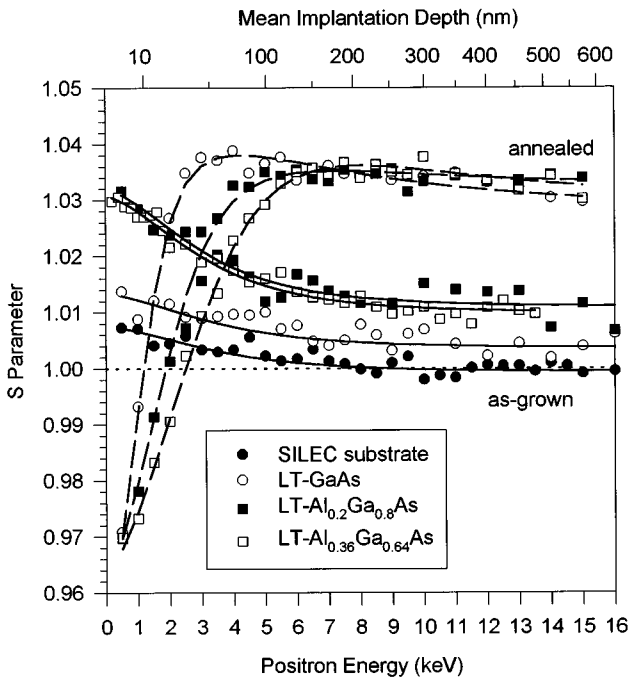

FIG. 7. S parameter vs positron implantation energy. Data are normalized to the substrate bulk S parameter value. The solid lines indicate the best fit to as-grown experimental data, while the annealed data are fitted with the dashed lines.

a uniform distribution of defects. Under arsenic-rich growth conditions, the predominant vacancy defect is group-III related,[18] and so the increased S parameter suggests that these defects (V_{Ga} and V_{Al}) are introduced in greater numbers during LT growth. The solid line fits produced by VEPFIT indicate a positron diffusion length (L) of 65(±10) nm for the substrate and LT-GaAs sample, and 55(±10) nm for the LT-$Al_xGa_{1-x}As$ samples. These values are much smaller than for undoped bulk GaAs (227 nm),[42] and in reasonable agreement with the work of Wei *et al.*,[18] who found positron diffusion lengths of ~36 nm. These low values of L can be attributed to an increased level of positron trapping and scattering due to the increased defect concentrations introduced during LT growth. The lower than normal value for the substrate control indicates that this wafer probably had also had a high level of defects, and it should be noted that Wei *et al.*[18] also encountered this anomalous behavior. Using these values for diffusion length (L), it is possible to calculate the concentration of defects [C_d] using

$$C_d = (k_{\text{eff}} - \lambda_f)/\mu_d, \tag{5}$$

where k_{eff} is given by $k_{\text{eff}} = D_+/L^2$, where D_+ is diffusion constant of positrons (taken as 1.6), λ_f is the free annihilation rate (232 ps^{-1}), and μ_d is the specific trapping rate (2.5×10^{15} s^{-1}). By this method the concentration of monovacancies in the as-grown LT layers is found to be between ~7 and 9×10^{17} cm^{-3}, which is in excellent agreement with the value of 3×10^{17} cm^{-3} reported by Keeble *et al.*[16]

After annealing, the normalized S parameter data for all three LT layers alter dramatically, as is also illustrated in Fig. 7. For positrons implanted deeper than ~0.1 μm, the S parameter values for all samples are almost the same (1.035)

Downloaded¬09¬Nov¬2006¬to¬147.8.21.97.¬Redistribution¬subject¬to¬AIP¬license¬or¬copyright,¬see¬http://jap.aip.org/jap/copyright.jsp

and are fairly constant, showing only a weak tendency to decrease with depth. In this region all samples exhibit an L value of 170($\pm$30) nm. However, in the subsurface region (0–0.1 μm), each of the LT layers has a very different profile, with a lowering of the S parameter for increasing Al mole fraction. The peak value for the normalized S parameter is found to be 1.04 at a depth of ~50 nm in the LT-GaAs layer. This is in good agreement with the work of others.[16] The best fits to the data (using a two-layer model) yield the following diffusion lengths: 35($\pm$5) nm for LT-GaAs, 65($\pm$10) nm for LT-$Al_{0.2}Ga_{0.8}As$, and 80($\pm$10) nm for LT-$Al_{0.36}Ga_{0.64}As$. For LT-GaAs grown at the same temperature, Hozhabri *et al.*[17] reported a positron diffusion length of 47 nm in the topmost 57 nm, which is consistent with our results.

The increase in the S parameter, and hence in the concentration of vacancy-related defects, upon annealing can be explained by the fact that the precipitates of arsenic that form are composed of As atoms diffusing from both antisite and interstitial positions. Clearly, the number of vacancy-type defects increases as the following reaction (for GaAs) proceeds

$$As_{Ga} \rightarrow As_{diff} + V_{Ga}, \tag{6}$$

where As_{Ga} is the arsenic atom in an antisite position, As_{diff} is the arsenic atom as it diffuses through the lattice, and V_{Ga} is the resulting gallium vacancy. However, as Hozhabri *et al.*[17] have stated, this would result in a larger but uniform distribution of V_{Ga}; instead we observe a large nonuniformity in the surface region. Furthermore, saturation trapping of positrons into monovacancies in GaAs[41] results in an increased S parameter of <2.5%, which is below the 3.5%–4% reported here. It is therefore believed that such high levels of positron trapping are due to divacancies or vacancy clusters. As annealing progresses, and the arsenic antisites vacate their lattice sites to form precipitates, the concentration of vacancy-related defects, [V], increases and eventually becomes so large that clusters form.

In a later work, Hozhabri *et al.*[43] investigated LT-GaAs using XPS and reported that there was a lower concentration of arsenic at the surface compared to deeper in the LT layer. Positron beam results showed that the depth profile of vacancy clusters followed an almost identical trend, which led these authors to conclude that these vacancy complexes were associated with the arsenic precipitates. However, the surface S parameter (S_{surf}) in their study was the same as the bulk value, whereas in our case S_{surf} can be seen to be ~3% below the bulk. Therefore, in order to explain this large decrease in S_{surf} we used XPS to examine the chemical profile in this region, and the results are shown in Fig. 8.

Probably the most striking feature of the XPS data is the dramatic reduction in arsenic at the surface of the samples, along with the concomitant penetration of oxygen. Unfortunately, this would seem to suggest that our annealing procedure was not ideal, and that some arsenic was able to escape from the surface allowing oxygen to diffuse in its place. Insufficient overpressure of forming gas would seem to be a likely cause for this phenomenon. Having said that, the different arsenic and oxygen profiles for the GaAs and $Al_xGa_{1-x}As$ films yield important information. Work by

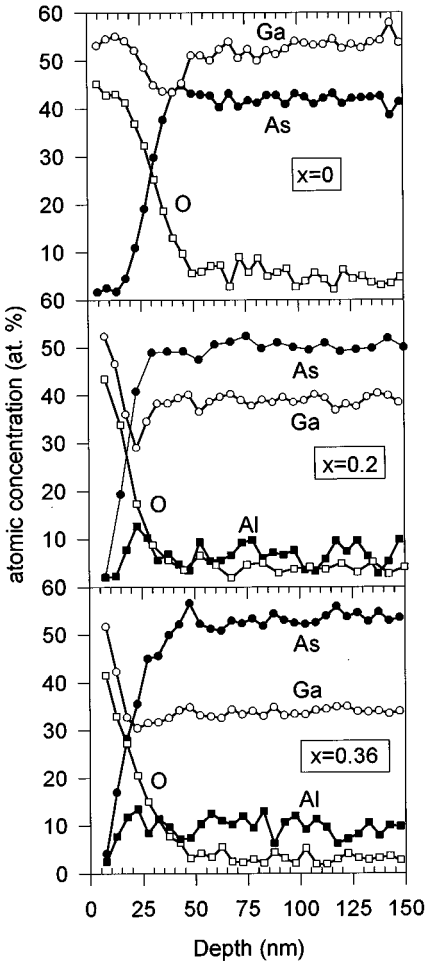

FIG. 8. XPS data for the three annealed samples (aluminum mole fraction of $x=0$, 0.2, and 0.36) showing atomic concentration (at. %) vs sputter depth.

Dannefaer and Kerr[44] has shown that a large reduction in the S parameter occurs at the surface due to the presence of oxygen. This then would explain why we see such a big change in S from the surface to the bulk (~7%). In addition, the oxygen penetrates deeper into the GaAs than into the $Al_xGa_{1-x}As$ layers; for GaAs the crossover point for the oxygen and arsenic curves is at ~30 nm, with the oxygen dropping below 5 at. % by ~50 nm. On the other hand, for $Al_xGa_{1-x}As$, the crossover is at ~15 nm and a level of 5 at. % is reached at a depth of ~35 nm. This would suggest that the presence of Al strengthens the gallium sublattice, allowing less excess arsenic to be incorporated during growth (as was seen in the x-ray data), and preventing as much oxygen penetration during annealing as for the LT-GaAs sample.

We believe that the XPS data also hold the key to understanding the differences in apparent positron diffusion length in the surface region of the annealed samples (Fig. 7). For LT-GaAs, the arsenic concentration does not reach its bulk value until ~45–50 nm below the surface. Therefore, the S parameter in this region is being dominated by the effect of a large concentration of oxygen, and the contribution from the positron trap centers is effectively masked. Beyond 50 nm the relatively flat S parameter is indicative of the divacancy/vacancy cluster concentration. However, for

Downloaded¬09¬Nov¬2006¬to¬147.8.21.97.¬Redistribution¬subject¬to¬AIP¬license¬or¬copyright,¬see¬http://jap.aip.org/jap/copyright.jsp

the $Al_xGa_{1-x}As$ samples the arsenic-deficient region only extends ~25–30 nm below the surface. Hence, except for the first few data points, the $Al_xGa_{1-x}As$ S parameter curves reflect the concentration of positron trap centers (monovacancies), and calculations using Eq. (5) show these to be 7×10^{17} cm^{-3} for $x=0.2$ and 4×10^{17} cm^{-3} for $x=0.36$.

As previously stated, the predominant vacancy-related defect in such arsenic-rich material is group-III related. If the Al–As bond is stronger than the Ga–As bond, we might expect that the concentration of gallium vacancies $[V_{Ga}]$ exceeds the concentration of aluminum vacancies $[V_{Al}]$. Annealing studies by Bliss *et al.*[20] led to the concept of V_{Ga}-enhanced diffusion of As_{Ga} defects. Similarities between LT-GaAs and neutron-irradiated GaAs (such as large numbers of V_{Ga} and rapid annealing time for As_{Ga}-related defects) pointed to the diffusion mechanism

$$As_{Ga1}+V_{Ga2}\leftrightarrow As_{Ga2}+V_{Ga1}, \tag{7}$$

with 1 and 2 being the nearest neighbor Ga sites. The mobile V_{Ga} allow for As_{Ga} diffusion by acting as ''arsenic sinks.'' Since $[V_{Ga}]$ in the LT layers is ~10^3 times greater than $[V_{Ga}]$ in an undoped semi-insulating substrate material,[20] only migration energy need be supplied for As precipitation (i.e., As_{Ga} diffusion) to begin. On the other hand, diffusion of As_{Ga} in bulk GaAs can only occur if there is additional energy for vacancy creation. This accounts for the disparity in As_{Ga}-annealing temperature between the LT layers (~500 °C) and bulk GaAs (>1000 °C). Using this model, it can be argued that for our samples As_{Ga} diffusion proceeds the slowest in LT-GaAs (highest $[As_{Ga}]^0$, lowest $[V_{Ga}]$), faster for $x=0.2$ (same $[As_{Ga}]^0$, higher $[V_{Ga}]$), and fastest in $x=0.36$ (lowest $[As_{Ga}]^0$, highest $[V_{Ga}]$). Now, if as Hozhabri *et al.*[43] have suggested, the vacancy clusters are associated with arsenic precipitates, then this difference in the rate of arsenic precipitation should be observable in the different S parameter profiles for the LT-$Al_xGa_{1-x}As$ beyond ~25 nm from the surface (away from the oxygen effects). Indeed, in the LT-$Al_{0.36}Ga_{0.64}As$ the formation of vacancy clusters has proceeded faster than in the LT-$Al_{0.2}Ga_{0.8}As$ sample, resulting in a lower concentration of monovacancies (and lower S) in the rising part of the curves before the saturated S parameter for the bulk vacancy clusters dominates. Further annealing studies of LTMBE-grown $Al_xGa_{1-x}As$ are planned.

IV. CONCLUSIONS

We have studied both GaAs and $Al_xGa_{1-x}As$ grown at low temperature using a variety of techniques in order to characterize their structural and defect properties. We have shown that the lattice expansion associated with this type of growth is smaller in the $Al_xGa_{1-x}As$ layers than for GaAs, indicating that excess arsenic incorporation is inhibited due to the presence of aluminum. Annealing at 600 °C is sufficient to redistribute the excess arsenic such that the increased lattice parameters return to their ''normal'' values. $[As_{Ga}]^0$ concentrations in the as-grown layers show almost no change as a function of Al mole fraction, revealing that the presence of Al does not significantly affect this type of defect. After annealing the $x=0$ and $x=0.2$ layers both show a decrease in $[As_{Ga}]^0$ of ~65%, whereas for the $x=0.36$ layer the decrease is much larger (~35%), indicating that for large Al mole fractions the formation of arsenic precipitates proceeds more slowly. Positron beam measurements show that the concentration of vacancy-type defects is greater in the as-grown LT-$Al_xGa_{1-x}As$ layers than for as-grown LT-GaAs. After annealing the bulk (i.e., deeper in the LT layer than ~150 nm) the S parameter value had increased by ~4%, indicating the presence of divacancies or vacancy clusters. X-ray photoelectron spectroscopy reveals that arsenic outdiffusion occurred during annealing (being replaced by oxygen), which we attribute to an insufficient overpressure of forming gas. The extra peaks that we observe for the annealed layers (at 200 and 257 cm^{-1}) are thought to be associated with disorder in this region. Oxygen penetration was greater (i.e., deeper) in the LT-GaAs layer than in the LT-$Al_xGa_{1-x}As$ layers, and this causes the very large lowering of the S parameter (~3%) at the surface. Further away from the surface, as the oxygen effects are reduced, we find evidence for a faster rate of vacancy cluster formation in the $x=0.36$ layer than in the $x=0.2$ layer, consistent with the vacancy-enhanced As_{Ga} diffusion model.

ACKNOWLEDGMENTS

It is a pleasure to acknowledge the assistance of Wesley R. Nieveen, the Associate Director of the Materials Characterisation and Preparation Centre (MCPC) of the Hong Kong University of Science and Technology, for making the x-ray, FTIR, XPS, and Raman facilities available for this work. Thanks also go to Y. F. Hu and C. V. Reddy of the Department of Physics, University of Hong Kong.

[1] M. Kaminska, Z. Liliental-Weber, E. R. Weber, T. George, J. B. Kortright, F. W. Smith, B.-Y. Tsaur, and A. R. Calawa, Appl. Phys. Lett. **54**, 1881 (1989).
[2] J. P. Ibbetson, J. S. Speck, N. X. Nguyen, A. C. Gossard, and U. K. Mishra, J. Electron. Mater. **22**, 1421 (1993).
[3] N. D. Jäger, A. K. Verma, P. Dreszer, N. Newman, Z. Liliental-Weber, M. van Schilfgaarde, and E. R. Weber, J. Electron. Mater. **22**, 1499 (1993).
[4] F. W. Smith, H. Q. Lee, V. Diadiuk, M. A. Hollis, A. R. Calawa, S. Gupta, M. Frankel, D. R. Dykaar, G. A. Mourou, and T. Y. Hsiang, Appl. Phys. Lett. **54**, 890 (1989).
[5] M. Kaminska and E. R. Weber, Mater. Sci. Forum **83–87**, 1033 (1992).
[6] M. O. Manasreh, D. C. Look, K. R. Evans, and C. E. Stutz, Phys. Rev. B **41**, 10272 (1992).
[7] J. Haruyama, N. Goto and H. Negishi, Appl. Phys. Lett. **61**, 928 (1992).
[8] D. C. Look, Z.-Q. Fang and J. R. Sizelove, Phys. Rev. B **47**, 1441 (1993).
[9] T. Murotani, F. Shimanoe and S. Mitsui, J. Cryst. Growth **45**, 302 (1978).
[10] F. W. Smith, A. R. Calawa, C. L. Chen, M. J. Manfra and L. J. Mahoney, IEEE Electron Device Lett. **EDL-9**, 77 (1988).
[11] K. M. Yu, M. Kaminska, and Z. Liliental-Weber, J. Appl. Phys. **72**, 2850 (1992).
[12] K. Zhang and D. L. Miller, J. Electron. Mater. **22**, 1433 (1993).
[13] Z. Liliental-Weber, K. M. Yu, J. Washburn, and D. C. Look, J. Electron. Mater. **22**, 1395 (1993).
[14] M. Fatemi, B. Tadayon, and M. E. Twigg, Phys. Rev. B **48**, 8911 (1993).
[15] X. Liu, A. Prasad, W. M. Chen, A. Kurpiewski, A. Stoschek, Z. Liliental-Weber, and E. R. Weber, Appl. Phys. Lett. **65**, 3002 (1994).
[16] D. J. Keeble, M. T. Umlor, P. Asoka-Kumar, K. G. Lynn, and P. W. Cooke, Appl. Phys. Lett. **63**, 87 (1993).
[17] N. Hozhabri, S. C. Sharma, R. N. Pathak, and K. Alavi, J. Electron. Mater. **23**, 519 (1994).
[18] L. Wei, Y. Tabuki, S. Tanigawa, D. E. Bliss, W. Walukiewicz, J. Ager, E. E. Haller, and K. Chan, Inst. Phys. Conf. Ser. **129**, 525 (1992).
[19] M. R. Melloch, N. Otsuka, J. M. Woodall, A. C. Warren, and J. L. Freeouf, Appl. Phys. Lett. **57**, 1531 (1990).

Downloaded¬09¬Nov¬2006¬to¬147.8.21.97.¬Redistribution¬subject¬to¬AIP¬license¬or¬copyright,¬see¬http://jap.aip.org/jap/copyright.jsp

[20] D. E. Bliss, W. Walukiewicz, J. W. Ager III, E. E. Haller, K. T. Chan, and S. Tanigawa, J. Appl. Phys. **71**, 1699 (1992).
[21] A. K. Verma, J. Tu, J. S. Smith, H. Fujioka, and E. R. Weber, J. Electron. Mater. **22**, 1417 (1993).
[22] K. Mahalingam, N. Otsuka, M. R. Melloch, J. M. Woodall, and A. C. Warren, J. Vac. Sci. Technol. B **10**, 812 (1992).
[23] A. K. Verma, J. S. Smith, H. Fujioka, and E. R. Weber, J. Appl. Phys. **77**, 4452 (1995).
[24] A. Prasad, X. Liu, P. Stallinga, E. R. Weber, A. K. Verma, and J. S. Smith, Mater. Res. Soc. Symp. Proc. **378**, 213 (1995).
[25] S. Adachi, in *GaAs and Related Compounds: Bulk Semiconducting and Superlattice Properties* (World Scientific, Singapore, 1994), p. 15.
[26] M. Missous (private communication).
[27] G. M. Martin, Appl. Phys. Lett. **39**, 747 (1981).
[28] A. Halec, P. Maguire, P. J. Simpson, P. J. Schultz, G. C. Aers, T. E. Jackman, and P. Marshall, Proceedings of the 5th International Workshop on Positron Beam Studies of Solids and Surfaces, SLOPOS-5, Jackson Hole, WY, 1992.
[29] P. J. Schultz and K. G. Lynn, Rev. Mod. Phys. **60**, 701 (1988).
[30] K. Mahalingam, N. Otsuka, M. R. Melloch, and J. M. Woodall, Appl. Phys. Lett. **60**, 3253 (1992).
[31] R. Ashokan, K. P. Jain, H. S. Mavi, and M. Balkanski, J. Appl. Phys. **60**, 1985 (1986).
[32] R. S. Berg, N. Mavalvala, and T. Steinberg, J. Electron. Mater. **19**, 1323 (1990).
[33] P. D. Wang, C. Cheng, C. M. Sotomayor Torres, and D. N. Batcheldor, J. Appl. Phys. **74**, 5907 (1993).
[34] S. Adachi, in *Properties of Aluminium Gallium Arsenide* (Institute of Electrical Engineers, London, 1993).
[35] B. Jusserand and J. Sapriel, Phys. Rev. B **24**, 7194 (1981).
[36] S. O'Hagan and M. Missous, J. Appl. Phys. **75**, 1835 (1994).
[37] H. J. von Bardeleben, M. O. Manasreh, D. C. Look, K. R. Evans, and C. E. Stutz, Phys. Rev. B **45**, 3372 (1992).
[38] R. E. Pritchard, S. A. McQuaid, L. Hart, R. C. Newman, J. Mäkinen, H. J. von Bardeleben, and M. Missous, J. Appl. Phys. **78**, 2411 (1995).
[39] G. C. Aers, P. A. Marshall, T. C. Leung, and R. D. Goldberg, Proceedings of the 6th International Workshop on Positron Beam Studies of Solids and Surfaces, SLOPOS-6, Makuhari, Tokyo, 1992.
[40] A. van Veen, H. Schut, J. de Vries, R. A. Hakvoort, and M. R. Ijpma, AIP Conf. Proc. **218**, 171 (1990).
[41] E. Soininen, J. Mäkinen, P. Hautojärvi, C. Corbel, A. Freundlich, and J. C. Grenet, Phys. Rev. B **46**, 12394 (1992).
[42] C. C. Ling, T. C. Lee, S. Fung, C. D. Beling, H. M. Weng, J. H. Xu, S. J. Sun, and R. D. Han, J. Phys., Condens. Matter. **6**, 1133 (1994).
[43] N. Hozhabri, A. R. Koymen, S. C. Sharma and K. Alavi, in Ref. 39.
[44] S. Dannefaer and D. Kerr, J. Appl. Phys. **60**, 1313 (1986).

Downloaded¬09¬Nov¬2006¬to¬147.8.21.97.¬Redistribution¬subject¬to¬AIP¬license¬or¬copyright,¬see¬http://jap.aip.org/jap/copyright.jsp